Molecular Flow Resonance Raman Effect from Retinal and Rhodopsin†

R. H. Callender,* A. Doukas, R. Crouch,‡ and K. Nakanishi

ABSTRACT: We have performed resonance enhanced Raman measurements of retinal isomers in solution (all-trans, 11-cis, 9-cis, and 13-cis) and cetyltrimethylammonium bromide (CTAB) detergent extracts of bovine rhodopsin near physiological temperatures (17 °C). In order to measure these photolabile systems, we have developed a general technique which allows Raman measurements of any photosensitive material. This technique involves imposing a molecular velocity transverse to the Raman exciting laser beam sufficient to ensure that any given molecule moves through the beam so that it has little probability of absorbing a photon. We have also measured the resonance Raman spectra of crystals of the same retinal isomers. The data show that each isomer has a distinct and characteristic Raman spectra and that the spectrum of 11-*cis*-retinal is quite similar but not identical with that of rhodopsin and similarly for 9-*cis*-retinal compared with isorhodopsin. In agreement with previous work, the Raman data demonstrate that retinal and opsin are joined by a protonated Schiff base. Due to the fact that the Raman spectra of 11-*cis*-retinal (solution) and rhodopsin show bands near 998 and 1018 cm^{-1}, a spectral region previously assigned to C-Me stretching motions, it is suggested that 11-*cis*-retinal in solution is composed of a mixture of 12-s-trans and 12-s-cis, and that the conformation of rhodopsin is (perhaps distorted) 12-s-trans.

Rhodopsin is the visual pigment in disk membrane of vertebrate rod cells (Wald, 1968). It is composed of 11-*cis*-retinal linked to the glycoprotein opsin by a Schiff base. The opsin binding site accommodates many retinal isomers and retinal analogues (Ebrey et al., 1975) including 9-*cis*-retinal (Wald, 1967), the latter forming isorhodopsin. While much is known about the visible and near ultraviolet spectroscopic properties of rhodopsin and its photochemistry, very little is understood about the mechanisms responsible for its precise behavior or the conformation of 11-*cis*-retinal in the opsin matrix. For example, there are important questions pertaining to the cause of the considerable red shift in the absorption spectra of rhodopsin and its high quantum efficiency of isomerization compared to free retinals.

Resonance Raman spectroscopy (Tang and Albrecht, 1970) is a very promising new tool to probe an isolated part of a large macromolecular system, namely that part of the system which has an absorption band in resonance with the exciting irradiation. In this case the resonance enhanced spectra are due generally only to vibrational modes of the chromophore which couple to this absorption band. The technique has potentially wide applications to colored, macromolecular systems. Resonance Raman spectra have recently been obtained from several biologically interesting systems including free retinal (Rimai et al., 1971; Gill et al., 1971; Heyde et al., 1971), the purple membrane protein of *Halobacterium halobium* (Mendelsohn, 1973; Lewis et al., 1974; Mendelsohn et al., 1974) and bovine rhodopsin (Lewis et al., 1973; Oseroff and Callender, 1974; Mathies et al., 1976).

A major difficulty in measurements of the resonance Raman effect of the visual pigments or model compounds, however, is that they readily isomerize upon absorption of a photon. The Raman cross section is inherently small even in the resonance enhanced case; it can be on the order of nine orders of magnitude smaller than the absorption cross section for these molecules.[1] As we show below, it can not be assumed that ordinary stationary Raman experiments give rise to Raman results from samples which have not been photodegraded. The previous work of Oseroff and Callender (1974) recognized the extreme photolability of bovine rhodopsin by working at liquid nitrogen temperatures and, thus, were able to obtain photostationary (light intensity independent) Raman spectra of mixtures of rhodopsin, isorhodopsin, and prelumirhodopsin.

In this paper we develop a technique and analysis which can be used on these or other photosensitive samples in solution. It involves imposing a molecular velocity transverse to the Raman exciting laser beam sufficient to ensure that any given molecule moves through the laser beam faster than it has any significant probability of absorbing a photon. In this way the Raman apparatus detects essentially only the nonphotoisomerized pure starting material even though absorption is taking place. The photoisomerized molecules are simply removed from the laser beam faster than they can accumulate and are replaced by the original sample. Experimentally, this is accomplished by flowing the material through the laser beam in a capillary tube. This flow method for overcoming the difficulties of obtaining well-defined Raman spectra from photosensitive samples has also been

† From the Physics Department, City College of New York, New York, New York 10031 (R.H.C. and A.D.), and the Department of Chemistry, Columbia University, New York, New York 10027 (R.C. and K.N.). *Received November 18, 1975.* Work supported in part by a Cottrell Research Corporation grant, City University Research Award Program, and the National Science Foundation (BMS 75-03020), City College, and National Institutes of Health (EY 01253), Columbia University. R.C. was a National Institutes of Health postdoctoral fellow (EY 54237) during this study.

‡ Present address: Department of Ophthalmology, Medical University of South Carolina, Charleston, South Carolina 29401

[1] The ratio of the Raman to absorption cross sections at 568.2 nm for the ethylenic mode of rhodopsin is approximately 3×10^{-9} (unpublished data).

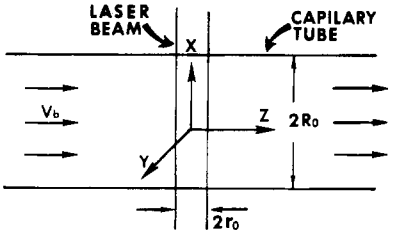

FIGURE 1: A schematic representation of the molecular flow experimental arrangement. The capillary tube is cylindrical with a radius of R_0. The arrows point along the direction of molecular flow. The y axis points toward the spectrometer.

recognized by Mathies et al. (1976) in their investigations of bovine rhodopsin and isorhodopsin. Other investigators have not explicitly considered this problem.

In the next section we develop the criterion needed to ensure that the Raman signal arises from starting material. The relevant parameters involved are the power of the incident laser beam, the absorption cross section at the frequency of the incident light, the laser beam diameter, and the flow velocity of the solution. We also derive expressions for the amount of necessary starting material.

We then apply this flow technique to obtain resonance enhanced Raman spectra arising solely from pure isomeric forms of retinal solutions (all trans, 11-cis, 9-cis, and 13-cis) and compare these results with those of CTAB[2] extracts of bovine rhodopsin near physiological temperatures (17 °C). We also present resonance Raman spectra of retinal crystals (all-trans, 11-cis, 9-cis, and 13-cis) as a comparison with their solution spectra. They are shown not to photoisomerize under the conditions that they are measured.

Molecular Flow Resonance Raman Technique

Conventional Stationary Raman Experiments. In typical Raman experiments, a laser beam is focused on a sample which is held in some sort of cell. For a molecule which is simultaneously absorbing photons, the number of photons per second absorbed is given by $I_0\sigma_A/\pi r_0^2$, where I_0 is the laser intensity (photons/s), so that $I_0/\pi r_0^2$ is the laser flux (photons/s cm^2), and σ_A is the molecular absorption cross section (cm^2/molecule) at the laser wavelength.[3] We are assuming for simplicity that the laser beam is circular with a radius of r_0 (cm). Thus, the mean time between successive molecular absorptions is the reciprocal of this number. Taking parameters relevant to rhodopsin, and using a laser wavelength at 568.2 nm at a power level of 10 mW and a beam radius of 40 μm, we find that a molecule will absorb a photon every 0.1 ms.

Of course, molecules in solution are not stationary. They are constantly moving in and out of the beam by diffusion and, if there is significant sample heating by the laser beam, by convection currents. To a first approximation, the molecular diffusion time (Broersma, 1960) to travel a distance r_0 is given approximately by $6\pi\eta d r_0^2/kT$, where η is the solvent viscosity, d the molecular "radius", k the Boltzmann constant, and T the absolute temperature. Taking d = 5 Å, $\eta = 10^{-2}$ P (for water), T = 300 K, r_0 = 40 μm, the transit time across the beam is 5 s. This assumes, of course, the best possible case, molecules are travelling transverse to the beam; molecular velocities parallel to the beam are just as possible. Obviously, a molecule will absorb many photons during its lifetime in the beam and in a time period which will not allow reliable Raman results.

Imposition of Molecular Flow. The basic idea in this technique is to replenish sample in the focused laser beam that has photoisomerized. Molecules in solution are made to travel transverse to the laser beam by a suitable pump. As they pass through the laser beam, some percentage of these molecules absorb light and some percentage of these will isomerize. As we will show here, it is a simple matter to arrange the flow characteristics so that a very small fraction of molecules in the laser beam has any probability of being isomerized. Since a molecule can independently either absorb a photon or scatter a Raman photon, the Raman measurement represents the original sample.

To calculate the fraction of molecules in the laser beam which are photoisomerized, we determine the probability that a given molecule in its transit through the laser beam will photoimerize. The experimental configuration for this calculation is given in Figure 1. Assume the flow direction is parallel to the z axis, and the laser light is parallel to the x axis. We assume the laser beam intensity profile is Gaussian (our case), and then the beam flux (photons/cm^2 s) in the yz plane is given by

$$F(\vec{r}) = \frac{I_0}{\pi r_0^2} e^{-\frac{(y^2+z^2)}{r_0^2}} \tag{1}$$

where r_0 is the distance to the $1/e$ points of the laser beam and can be taken to be the beam radius. This molecule will begin its transit along the z axis (flow direction) far from the beam center with a constant value of its y coordinate and constant velocity, v_b, so that $z = v_b t$. The probability of photoisomerization as a function of time is given by

$$P(y,t) = \sigma_A \psi \int_{-\infty}^{t} \left(\frac{I_0}{\pi r_0^2} e^{-\frac{(y^2+v_b^2 t'^2)}{r_0^2}}\right) dt' \tag{2}$$

where ψ is the quantum yield of photoisomerization. By extending the limit of the integral to infinity and taking y = 0, we obtain an expression for P_m, the total number of photons absorbed and causing photoisomerization of a molecule during a single transit through the *center* of the laser beam.

$$P_m = \frac{1}{\sqrt{\pi}} \frac{I_0 \sigma_A \psi}{r_0 v_b} \tag{3}$$

This number, by a suitable choice of experimental parameters, can be made much less than one. In fact, it can be made arbitrarily small by simply increasing the molecular velocity, v_b. It is for this reason that the molecular flow technique works. Very few molecules in the laser beam have photoisomerized, a necessary criterion for obtaining reliable Raman results.

We turn now to the more general and detailed problem of calculating the Raman scattering from photoisomerized sample, S', compared with that of nonphotoisomerized sample, S. The number of Raman events, S, detected at the photomultiplier per second, of a particular species with a concentration $C(\vec{r})$ (molecules/cm^2) and Raman cross section σ_R (cm^2/mol/steradian) is given by

$$S = \sigma_R \Omega_0 e_R \int_V F(\vec{r}) C(\vec{r}) dV \tag{4}$$

where Ω_0 is the solid angle (sr) subtended by the collecting lens of the apparatus and e_R the total efficiency of the Raman apparatus. We view the system as having two

[2] Abbreviation used: CTAB, cetyltrimethylammonium bromide.

[3] The absorption cross section is related to the molar extinction coefficient, ϵ, at a particular wavelength by $\sigma_A = 3.824 \times 10^{-21}\epsilon$.

species, photoisomerized and nonphotoisomerized material, with a total concentration of C_0. The probability that a molecule has photoisomerized is given by eq 2 provided this number is less than one. Elsewhere it is one. We are explicitly discounting, here, the possibility that a molecule may absorb more than one photon and finally photoisomerize back to the original sample. In a detailed calculation for rhodopsin, it would be necessary to take account of the kinetic lifetimes of the photointermediates. Once a molecule photoisomerizes, it is considered to give rise to spurious Raman scattering in our calculation.

It is convenient to rewrite the probability of photoisomerization in terms of the molecular position in the zy plane. From eq 2 and 3 this is given by

$$P(y,z) = P_m \frac{1}{\sqrt{\pi} r_0} \int_{-\infty}^{z/v_b} e^{-\frac{(z'^2 + y^2)}{r_0^2}} dz' \qquad (5)$$

where it is understood that $P(y,z)$ is given by eq 5 or unity, whichever is less. In this case $C(\vec{r}) = C_0(1 - P(y,z))$. Substitution of these concentrations into eq 4, performing the integrals, and assuming that $P(y,z)$ is always much less than one (so that $C(\vec{r}) \simeq C_0$), we find that

$$\frac{S'}{S} = \frac{\sigma_R'}{\sigma_R} \frac{P_m}{\sqrt{8}} \qquad (6)$$

By a suitable choice of the parameters which determine P_m (i.e., v_b, I_0, r_0, σ_A, and ψ), S'/S can be made as small as necessary.[4]

In the above calculation of S'/S, we have ignored any variation in the molecular flow velocities. It is well known, however, that the velocity profile for pipe flow is not uniform. In fact near the pipe walls the flow velocity tends to zero so that S'/S as given by eq 6 actually tends to infinity. We briefly consider the importance of a nonuniform velocity profile.

The type of flow velocity profile in pipes has been extensively studied. It is categorized by the so-called Reynold's number (Landau and Lifshitz, 1959)

$$K = \frac{2\rho v_b R_0}{\eta} \qquad (7)$$

where ρ and η are, respectively, the fluid density and viscosity and R_0 is the radius of pipe. For $K < 2000$, the fluid flow is said to be laminar and the velocity profile along the x axis is then

$$v(x) = \frac{2v_b}{R_0^2}(R_0^2 - x^2) \qquad (8)$$

where v_b is the average or bulk fluid velocity.[5] For $K > 3000$, the fluid is turbulent and the velocity profile, while not precisely known, is more uniform and equal to v_b across the pipe (Tennekes and Lumley, 1972). These divisions are somewhat arbitrary in that precise experimental conditions influence the point of onset and degree of turbulence. However, we can estimate the influence of the nonuniform flow velocity by considering laminar flow since this represents the worst possible case in its modification of S'/S.

The calculation proceeds as follows. Since the laser beam is very narrow in the zy plane, the velocity in this plane can be considered as constant. Thus in evaluating eq 4, the influence of the nonuniform flow is contained in performing the integral in the direction along the laser beam (the x axis). The x dependence is then contained in the concentrations, $C(\vec{r})$ and $C'(\vec{r})$, since $P(y,z)$ (see eq 5) is now dependent on the x coordinate by substituting the velocity profile of eq 8 into P_m. Remembering that $P(x,y,z)$ never exceeds one, the integrals can be performed exactly. In the case where P_m evaluated using v_b, i.e., $P_m(v_b)$ is much less than one, we find a simple approximate form for S'/S given by

$$\frac{S'}{S} = \frac{\sigma_R'}{\sigma_R} \frac{P_m(v_b)}{\sqrt{8}} \left[\frac{1}{4}\left(\ln \frac{8}{P_m(v_b)} + 1\right)\right] \qquad (9)$$

The effect of nonuniform flow is not very significant. For example, assuming $P_m(v_b) = 0.14$ and $\sigma_R'/\sigma_R = 1$, $S'/S = 0.05$ for uniform flow and 0.06 for laminar flow. It is clear that the ratio of Raman scattering from photoisomerized molecules to original sample, even allowing nonuniform flow, can be maintained at a very small value.

The key parameter in these flow measurements is the value of $P_m(v_b)$ which can be determined by separate measurements of I_0, σ_A, ψ, r_o, and v_b. The value of this parameter can, however, also be determined by measuring the percentage of photoisomerized sample after the entire sample has made a single transit through the laser beam. This percentage of photoisomerization, $\bar{P}$, is the average of $P(x,y,z)$ where $z = \infty$ (i.e., a single transit). We have

$$\bar{P} = \frac{\int\int_A P(x,y,\infty) dx dy}{\int\int_A dx dy} \qquad (10)$$

where the integral is to be evaluated over the area of the flowing sample. We find in the case of uniform flow that

$$\bar{P} = P_m(v_b) \frac{2}{\sqrt{\pi}} \frac{r_0}{R_0} \qquad (11)$$

and in the case of a laminar flow pattern that

$$\bar{P} = P_m(v_b) \frac{2}{\sqrt{\pi}} \frac{r_0}{R_0} \left[\frac{1}{4}\left(\ln \frac{8}{P_m(v_b)} + 1\right)\right] \qquad (12)$$

to a good approximation. Thus a measurement of $\bar{P}$ gives an independent check on the value of $P_m(v_b)$.

Necessary Starting Sample. At all times molecules are undergoing photoisomerization; as such they are effectively destroyed. We calculate in this section an expression for the amount of necessary starting sample.

$\bar{P}$ of eq 10, the fraction of photoisomerized sample, is a measure of how the sample is being degraded as photons are absorbed. We are used to thinking of the sample photoisomerization as a function of time; therefore, instead of using eq 10, we derive $\bar{P}$ in a more traditional sense. If A is the absorbance of the sample, then $I_0(1 - 10^{-A})$ represents the total number of photons/s that are absorbed by the sample. The total number of molecules in the sample is given by C_0V, where V is the total sample volume. We then have

$$\bar{P} = \frac{I_0[1 - 10^{-A}]T}{C_0 V} \psi \qquad (13)$$

where T is the time of the Raman measurement. We are assuming a molecule has a small probability of absorbing a

[4] Although derived from a very different approach, the result of Mathies et al. (1976) is in complete agreement with eq 6 when this expression is written in an equivalent form to theirs.

[5] The bulk velocity is generally defined as the average of the velocity profile transverse to the flow axis, i.e., $v_b = \int\int_A v(x,y)\, dx dy / \int\int_A dx dy$, where the integration is over the area of the pipe.

photon which is the case if P_m and $\bar{P}$ are small. If A is small, then by expanding the exponential in eq 10

$$\bar{P} = \frac{2.3 I_0 A T \psi}{C_0 V} \tag{14}$$

There are advantages to making the absorbance small (which can be controlled by suitable choice of the laser frequency) since (1) there is some evidence that the resonance Raman cross section drops more slowly than the absorption cross section as the laser frequency moves away from the absorption maxima of the sample (Fenstermacher and Callender, 1974) and (2) the scattered Raman light is then not strongly attenuated in exiting from the sample.

The time for the Raman measurement, T, can be readily calculated in terms of the Raman cross section. The number of detected Raman events, S, is given by eq 4. Assuming that essentially all the sample in the laser beam profile is pure starting sample, we have

$$S = I_0 \sigma_R \Omega_0 e_R l C_0 \tag{15}$$

where l is the path length of the laser beam in the sample ($2R_0$ in our geometry but more precisely the length of laser beam actually detected). It should be noted that all quantities except Ω_0 and l are functions of the laser wavelength. We are assuming that the laser light is not appreciably absorbed by the sample so that I_0 is constant along the entire beam and also that the entire incident beam profile contributes to the Raman scattering. We now need to develop a criterion for the total number of detected Raman events necessary. If we call this parameter N, the $TS = N$. Using the language of modern photon counting techniques, the entire Raman spectrum can typically be stored in 500 "channels" and each channel would contain 10^3 detected Raman events for a noise-to-signal ratio of 0.03 assuming that there is no background fluorescence or photomultiplier noise; then $N = 5 \times 10^5$. Combining eq 14 and 15 and remembering that absorbance is given by

$$A = \frac{\sigma_A C_0 l}{2.3} \tag{16}$$

We then find that

$$\bar{P} = \frac{\sigma_A}{\sigma_R} \psi \frac{N}{\Omega_0 e_R C_0 V} \tag{17}$$

The fraction of the sample that is photoisomerized during the Raman experiments depends essentially on the ratio of absorption to Raman cross sections, the number of Raman events that are detected, and inversely on the total number of molecules in the sample. Although $\sigma_A N/\sigma_R$ may be on the order of 10^{14}, $\bar{P}$ can be made arbitrarily small by simply increasing the total number of molecules in the sample.

For rhodopsin, assuming a ratio of $\sigma_A/\sigma_R = 3 \times 10^8$ for all Raman lines,[1] $\psi = 0.67$, $\Omega_0 = 1$, $e_R = 0.01$, and $N = 5 \times 10^5$, we find that, to require $\bar{P}$ to be 0.01, it is necessary to have 170 ml of 10^{-5} M solution. Our typical experiment was with much larger quantities of material largely because of a fairly strong background fluorescence and because the weaker Raman structure has a substantially smaller Raman cross section than the ethylenic mode.

Methods and Materials

Laser Raman spectra were obtained with a Spex 1401 double monochrometer, a cooled RCA 31034 photomultiplier, and photon counting electronics interfaced to a PDP-8e minicomputer. Part of the memory of this computer was reserved for data storage in discreet channels. The PDP-8e computer was in turn interfaced to a PDP-10 computer for general data storage and smoothing. A Coherent Radiation Model 52 krypton ion laser was used to produce the exciting irradiation. Three lines of this laser were used: the 520.8 nm lines at a power level of 1 mW for the molecular flow Raman data of retinal solutions; the 568.2 nm line at a power level of 10 mW for the molecular flow Raman data of rhodopsin; and 647.1 nm irradiation at a power level of 10 mW for the retinal crystals. All power levels were measured just before the sample with a calibrated Eppley thermopile. The spectrometer was calibrated by the known Kr^+ laser lines; line assignments are accurate to within ± 2 cm^{-1}. All the spectra presented here consist of digitally pooled data from multiple runs and all identified lines have been observed in several separate measurements. A typical single scan consisted of a spectrometer speed of 50 cm^{-1}/min and a channel dwell time of 2.2 s (an effective time constant of approximately 12 s) for a total of 512 channels.

The molecular flow apparatus consisted of a closed recirculating flow system driven by a small variable speed pump, Micro-pump Model 12-41-303. Sample temperature was maintained at 17 °C by immersing the sample reservoir in an ice bath. The capillary tube which intersected the exciting laser beam was the drawn end of a Pasteur pipet, having an internal diameter of 1.5 mm. The velocity of the fluid in the capillary tube was measured by determining the bulk flow velocity.[5] A typical value for the bulk flow velocity was 500 cm/s. The incident laser beam was defocused on the capillary tube producing a $1/e$ beam radius of 40 ± 5 μm as the capillary tube. The beam diameter and profile were determined by measuring the Rayleigh scattering of the flowing fluid with 10-μm spectrometer slits while moving the laser beam transverse to the spectrometer in known amounts. The magnification (×5.2) of the sample to spectrometer imaging lens was determined by replacing the sample with a microscope reticule and repeating the process. The beam diameter parallel to the beam axis was found not to vary by more than a few percent inside the capillary tube.

The ratio of Raman scattering from photodegraded sample to that of pure starting sample, S'/S, was determined from $P_m(\upsilon_b)$ in eq 9 by measuring I_0, σ_A, υ_b, and r_0, taking a value of $\psi = 0.67$ for rhodopsin, assuming $\psi = 1.0$ for all the retinals and assuming $\sigma'/\sigma = 1$. For rhodopsin, $P_m(\upsilon_b) = 0.14$ which gives $S'/S = 0.06$. As an independent check of $P_m(\upsilon_b)$, the percentage of photoisomerized rhodopsin after a single transit through the laser beam, $\bar{P}$, was measured under conditions otherwise identical with those of the Raman runs. $\bar{P}$ depends on $P_m(\upsilon_b)$ as given by eq 11 assuming uniform flow or eq 12 assuming laminar flow; the predicted value of $\bar{P} = 0.008 \pm 0.002$ from eq 11 and $\bar{P} = 0.010 \pm 0.002$ from eq 12 using $P_m(\upsilon_b) = 0.14$. The measured value, $\bar{P} = 0.009 \pm 0.003$, is quite consistent. For the retinal isomers, S'/S was much lower, less than 0.001 in all cases, since the exciting laser irradiation was considerably far from their absorption maxima. Thus, the Raman results presented here arise from the pure starting material with very small or negligible contributions from light-induced sample changes.

Rod outer segments were prepared from a recipe of Papermaster and Dreyer (1973) using bovine retinae purchased from Hormel (Austin, Minnesota). The rod outer segments were extracted in a solution of 1% CTAB, 67 mM potassium phosphate buffer at pH 6.5, and 100 mM hydroxylamine. This was then diluted with the same solution without

CTAB reaching approximately a 0.2% CTAB concentration and 150 ml at 10^{-5} M of extracted rod outer segments. The retinals other than 11-cis were obtained commercially from Sigma and used without further purification; the 11-cis isomer was a gift from the Hoffmann-La Roche company. Assays of the retinals were determined by high-pressure liquid chromatography (Chan et al., 1974) under the following conditions: Waters ALC-100, μ-Porasil, one or two 1 ft × 0.25 in. column(s), 1–4% ether/*n*-hexane (v/v), 1–2 ml/min flow rate, 350-nm detector. It was found that the all-trans and 13-cis were better than 97% pure, 11-cis 95% pure, and 9-cis 87% pure. A typical concentration of the retinal carbon tetrachloride solutions was 5 mM.

The solutions of retinals and rhodopsin were assayed for sample composition before and after each flow experiment. For rhodopsin, the decrease of the 500-nm absorption band was taken as a measure of the photobleaching of the sample.

There was considerable bleaching of the rhodopsin samples during the course of the experiment (i.e., many separate runs); however, because of the relatively high number of molecules, it was found that the degree of total photoisomerization in the retinal experiments was very small (less than 2%). The procedure during the flow experiments of rhodopsin was to acquire the Raman data until the sample was approximately 50% bleached. The entire sample was then completely bleached and separate Raman measurements were performed under identical conditions. It was found that the totally bleached sample gave a negligible Raman signal apart from a broad background fluorescence, and a small broad band near 1650 cm^{-1}, which is a well-known water line. We conclude that no significant Raman structure of retinaldehyde oxime is contained in the results. This spectrum was subtracted from the rhodopsin spectrum thus leaving a pure rhodopsin spectrum without background. The rate of formation of retinaldehyde oxime was monitored by measuring the absorbance increase at 365 nm after a bleaching pulse of light. It was found that this time was faster than the molecular round trip transit time in the rhodopsin flow experiments. Thus no significant Raman scattering of intermediate rhodopsin photoproducts is contained in the data. The carbon tetrachloride Raman scattering in the retinal solution data has also been subtracted out by separate Raman measurement of pure carbon tetrachloride.

The crystal Raman data were obtained by defocusing the 647.1-nm laser beam to completely illuminate the crystals. The sample was assayed after the Raman experiment. No change in isomeric composition was observed in all cases.

Results

Retinals. Figure 2 shows the molecular flow resonance Raman spectra of solution of all-*trans*-, 13-*cis*-, 9-*cis*-, and 11-*cis*-retinal isomers. From the previous work of Rimai et al. (1971) and Warshel and Karplus (1974), general spectral assignments can be made. The lines near 1670 cm^{-1} arise from the C=O stretching vibration. The largest structure in the spectra, near 1580 cm^{-1}, is assigned to the C=C stretching motions of the retinal polyene chain. From the standpoint of conformational information, the so-called fingerprint region around 900–1450 cm^{-1} is the most interesting. Changes in this region appear to be most sensitive to conformation. These bands consist chiefly of admixtures of C–C stretching and C–H bending modes. Structure near 1010 cm^{-1} has been assigned to the stretching mode between the methyl groups and the polyene chain, and bands near 1440 cm^{-1} to C–H bending within these methyl groups (Rimai et al., 1971; Warshel and Karplus, 1974). Other mode assignments in the fingerprint region are difficult to assign precisely since they represent group modes along the polyene chain; definitive mode assignments have not yet been made.

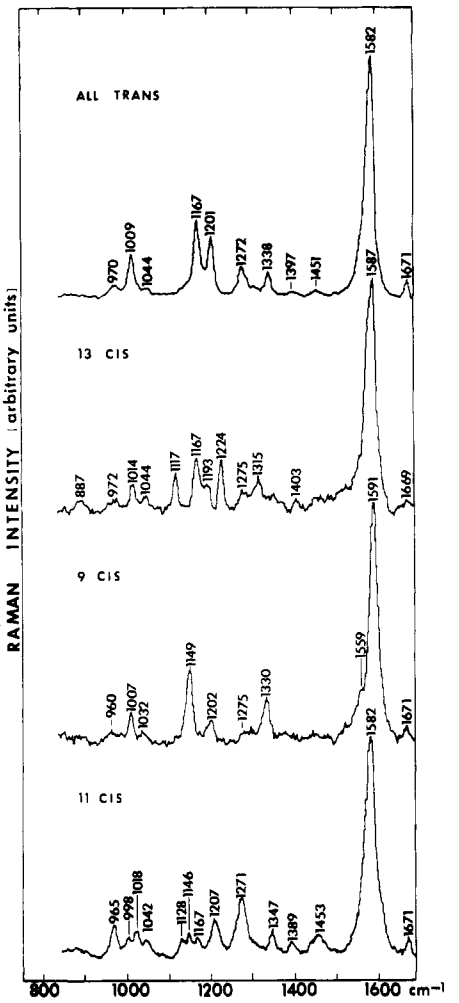

FIGURE 2: Resonance Raman spectra of various retinal isomers dissolved in carbon tetrachloride. The exciting laser frequency is 520.8 nm, and the resolution in all cases is 12 cm^{-1}.

A comparison of the data in Figure 2 shows that the Raman spectra are indeed very sensitive to conformation. For example, the structural difference between all-trans and 13-cis is not too large; yet, while there are similarities between the two spectra, there are significant differences. The lines at 970, 1010, 1167, 1201, and 1272 cm^{-1} repeat in both spectra. However, the 13-cis spectrum has lines at 1117, 1224, 1315 cm^{-1} not found in that of the all-trans; in all-trans, the 1338 cm^{-1} band is quite prominent compared with that of 13-cis. Similar comparisons among the other isomers in Figure 2 show significant changes in Raman structure correlated with isomeric form. The molecular flow resonance Raman measurements of Figure 2 are in agreement with previous published Raman measurements of these retinals (Rimai et al., 1971; Gill et al., 1971) excepting for small differences which presumably reflect some partial photoisomerization in those stationary measurements.

Figure 3 shows the Raman spectra of the same four forms as crystals. Compared with the solution spectra, the

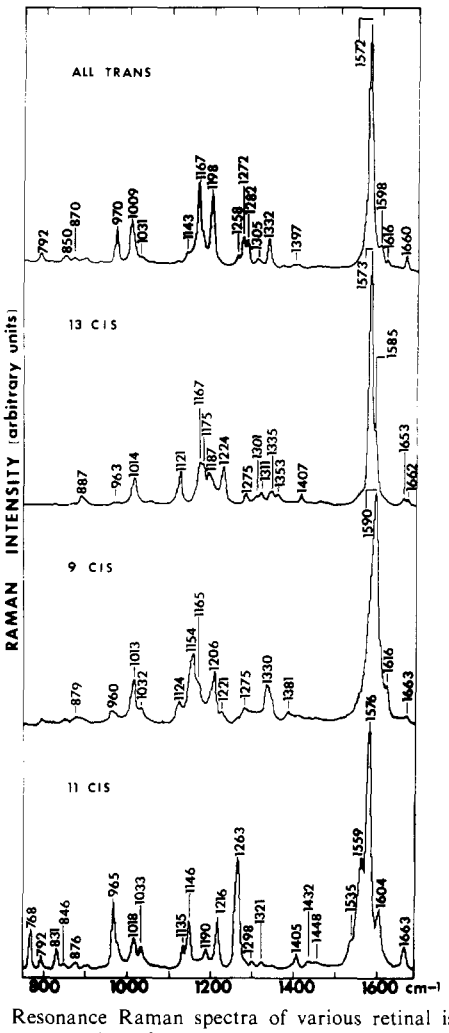

FIGURE 3: Resonance Raman spectra of various retinal isomers as crystals. The exciting laser frequency is 647.1 nm, and the resolution in all cases is 8 cm^{-1}.

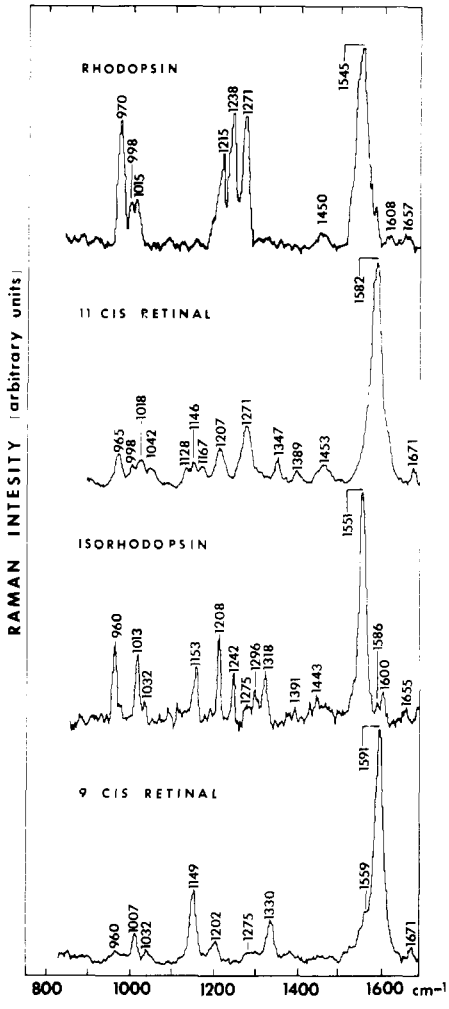

FIGURE 4: Resonance Raman spectrum of CTAB extracts of bovine rhodopsin taken with 568.2 nm exciting laser irradiation at a resolution of 10 cm^{-1}. The spectra of 11-*cis*- and 9-*cis*-retinal in solution (same as that of Figure 2) and isorhodopsin [reprinted with permission from Oseroff and Callender (1974), *Biochemistry 13*, 4243] are given for comparison purposes.

bands are generally sharper. It is apparent that many of the bands found in the solution spectra are really composed of separate nearly degenerate lines. This is perhaps most apparent in the C=C band of the 11-*cis*-retinal. In the crystal spectra, four separate lines are seen. That there are four C=C bands is not surprising since there are four C=C bonds in the polyene part of the retinal. These four bonds can be expected to form four different C=C group stretching modes which are close in energy to each other and would presumably have different Raman cross sections (Warshel and Karplus, 1974). In fact, the measured line positions (1535, 1559, 1576, and 1604 cm^{-1}) are in good agreement with the calculated values of Warshel and Karplus (1974) of 1565, 1646, 1660, and 1680 cm^{-1} after allowing that the potential surfaces used in the calculations have overestimated the C=C frequencies by about 80 cm^{-1}. It should be noted that to the extent that the C=C bond of the β-ionone ring moiety of retinal gives rise to a resonance enhanced Raman cross section, five separate C=C stretching modes could be observed in this spectral region. In the solution spectra, these line are either broadened or their line positions and Raman cross sections are changed so that they are often not separately resolved.

A comparison of the solution and crystal data in the fingerprint region reveals general similarities but some significant differences. As a general trend, the all-trans solution and crystal spectra are nearly identical but larger spectral differences appear in the other isomers. These differences presumably reflect different interactions that a retinal molecule may have with its surroundings in solution compared with its crystal host and/or differences in conformations. A very important observation in the spectra of 11-*cis*-retinal, an aspect which is discussed more fully below, is the appearance of two lines in the spectral region assigned to C-Me stretching, at 998 and 1018 cm^{-1}, in solution (Figure 2) as compared with a single 1018 cm^{-1} scattering line in the crystalline state (Figure 3).

Rhodopsin. Molecular flow resonance Raman spectra from CTAB detergent extracts of rhodopsin at 17 °C are shown in Figure 4. For comparison purposes, the 11-cis solution data are also repeated in this figure. In addition, the spectra of pure isorhodopsin taken from the previous low-temperature measurements of Oseroff and Callender (1974) are given along with the 9-*cis*-retinal solution data (same as Figure 2). This is a very important figure since, in principle, a detailed analysis of the Raman structure would lead to an understanding of the retinal conformation and environment in the opsin cavity for rhodopsin and isorhodopsin.

The rhodopsin spectrum contains lines at 970, 998, 1015, 1215, 1238, 1271, and 1450 cm^{-1} in the fingerprint region.

Except for small changes in position, all these lines, *except the 1238 cm^{-1} band,* are repeated in the 11-*cis*-retinal spectrum. However, there are generally more lines in the 11-*cis*-retinal spectrum: the two lines in the 1100–1200 cm^{-1} region[6] and a line at 1389 cm^{-1}. The C=C band in rhodopsin lies at 1545 cm^{-1}. The band at 1657 cm^{-1} is in close agreement with the position of a protonated Schiff base (C=NH$^+$) stretching frequency (Heyde et al., 1971).

The rhodopsin spectrum is in close agreement with that obtained by Mathies et al. (1976) from bovine rhodopsin in Ammonyx LO detergent solutions and in sonicated retinal disc membranes who also use a flow technique. However, the data are quite different from those obtained by Lewis et al. (1973) in their stationary Raman measurement suggesting substantial light-induced sample changes.

The spectrum of isorhodopsin is more complex than that of rhodopsin but appears to bear a close resemblance to that of 9-*cis*-retinal. Apart from differences in line width and position, the major difference between these two spectra is the appearance of a new line at 1242 cm^{-1} and the enhanced relative intensity of the 960 cm^{-1} band in isorhodopsin as opposed to 9-*cis*-retinal.

Discussion

Resonance Raman Spectra of Retinals. The data (Figures 2 and 3) indeed show that Raman spectra are quite sensitive to the molecular shape of retinals indicating that a detailed analysis of the data, in particular the fingerprint region of 900–1450 cm^{-1}, should provide valuable information on their conformations and intermolecular interactions.

In past resonance Raman studies of retinals and rhodopsin, much has been made of the inverse linear correlation between the C=C stretching frequency and the position of the absorption maximum of a particular species. For example, Oseroff and Callender (1974) found the C=C frequency decreasing almost linearly from 1563 cm^{-1} in protonated retinylidenethanolamine (λ_{max} 443 nm) to 1551 cm^{-1} in isorhodopsin (λ_{max} 494 nm) to 1539 cm^{-1} in bathorhodopsin (λ_{max} 543 nm). This type of correlation can be understood by considering that the cause of the bathochromic shift is due to an increased delocalization (from whatever causes) of the electrons of the polyene chain which decreases the force constant of the C=C band (Abrahamson and Wiesenfeld, 1972; Heyde et al., 1971; Honig and Ebrey, 1974).

However, it is clear from the data of Figure 2 that the double bond configurations can also play an important role in determining the observed C=C stretching frequency. The absorption maxima of these isomers in carbon tetrachloride are all-trans (383 nm), 13-cis (376 nm), 9-cis (375 nm), and 11-cis (378 nm). It can be seen from an inspection of Figure 2 that the correlation model is not particularly obeyed; the 11-cis C=C mode is, for example, anomalously low being equal to that of all-trans. (See also Gill et al. (1971) for a similar conclusion.)

A very important result is the observation of two lines at 998 and 1018 cm^{-1}, a spectral region which has been assigned to the C-Me stretching motions in the 11-cis solution spectrum (Figure 2). The appearance of two lines in this region is not found in any other solution or crystal spectrum including 11-cis crystal data (Figure 3).

A reasonable explanation of this is to assume that the 9- and 13-Me groups in the 11-cis, 12-s-cis (probably distorted) conformers (Figure 5b) both have stretching motions at 1018 cm^{-1} due to their similar environments (there should be no steric hindrance in either Me or in this conformation). In contrast we suggest that the two Me's in the 12-s-trans (probably distorted) conformers (Figure 5a) scatter at different frequencies, i.e., 9-Me at 1018 cm^{-1} and 13-Me at 998 cm^{-1},[7] because the former is not hindered while the latter is hindered. Steric interactions between the 13-Me and 10-H can certainly play a factor in this removal of degeneracy. It is known from x-ray diffraction studies (Gilardi et al., 1972) that crystalline 11-*cis*-retinal adopts a single distorted 12-s-cis structure. This is consistent with the appearance of a single Raman band at 1018 cm^{-1} in the cystalline data (Figure 4). It should be noted that the 13-Me/10-H interaction only plays a role in 11-*cis*-retinal; the C-Me stretching vibrations of the other isomers presented here would very likely remain degenerate or nearly degenerate whether or not there were significant deviations from a trans geometry along the C-12 single bond since the 13-Me is involved with little if any steric hindrance in these cases.

It is difficult to quantitatively determine the percentage of 11-cis, 12-s-trans relative to 11-cis, 12-s-cis present in solution from the data presented here since, at this time, the relative Raman cross section of the 9- and 13-Me stretching motions is unknown. The simplest assumption is that they have roughly equal Raman cross sections. In this case, the fact that in the 11-cis spectrum the 998 cm^{-1} band (due to 13-Me in 12-s-trans form) is less intense than the 1018 cm^{-1} (due to 9-Me in both forms plus 13-Me in 12-s-cis form) suggests that the isomer is in equilibrium between a 12-s-cis and 12-s-trans forms. The Raman intensity results, thus seen, would be an average resulting in a more intense 1018 cm^{-1} band than 998 cm^{-1} band.

This conclusion is in agreement with the theoretical calculation of Honig and Karplus (1971) and recent nuclear magnetic resonance measurements of 11-*cis*-retinal in solution by Rowan et al. (1974), both of whom conclude that the difference in energy between 12-s-cis and 12-s-trans forms is less than 1 kcal/mol, and that both forms may exist in equilibrium.

However, this conclusion conflicts to some extent with absorption and circular dichroism (CD) studies of model 14-methylretinals and pigments formed from them (Chan et al., 1974; Ebrey et al., 1975). Their conclusions are based on the assumption that the mere replacement of 14-H for a 14-Me group in 11-*cis*-retinal should not appreciably change the λ_{max} and, in view of the 14-Me/10-H steric interactions, this substitution should force the conformation away from 12-s-cis. They found that the λ_{max} (in EtOH) of 11-*cis*-14-methylretinal was weaker and considerably blue shifted (350 nm, ϵ 19 000) in comparison with 11-*cis*-retinal (375 nm, ϵ 26 000) and from this it was concluded that the 12-s-trans shape (distorted) is not the predominant form for 11-*cis*-retinal in solution. However, due to the broadness of the 11-*cis*-retinal 375 nm peak, their studies do not preclude the possibility of a significant percentage of the 12-s-trans form being present. We thus believe that the present results can be reconciled with the previous uv/vis spectral data by assuming that 11-*cis*-retinal in solution ex-

[6] We believe it is likely that the small line in the 11-*cis*-retinal spectrum (Figure 2) at 1167 cm^{-1} is an artifact arising from a small amount of *all-trans*-retinal present in the original sample.

[7] Gill et al. (1971) conjectured from their Raman 11-*cis*-retinal solution data that the two methyl stretching frequencies are different in 11-*cis*,12-*s*-*trans*-retinal.

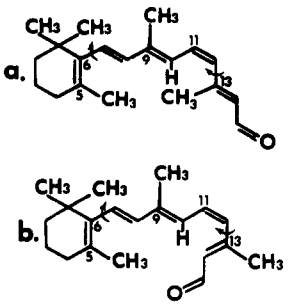

FIGURE 5: Two conformations of 11-*cis*-retinal as (a) 12-s-trans and (b) 12-s-cis.

ists as an equilibrium mixture between 12-s-cis and 12-s-trans, the exact composition to be determined by further studies.

Our interpretation of the line assignments of the C–Me stretching frequencies given above is a simple model of what could be a much more complex situation in terms of a detailed mode analysis. The stretching frequency of the C(5) methyl group can also be in this spectral region and can have significant Raman intensity (M. Karplus, private communication). Generally speaking, it can be expected that three lines would be seen in the results which would involve coupled normal modes that are combinations of stretching motions of these methyl groups (with varying degrees of contribution). In addition, contributions of other atomic motions of retinal could be coupled to the methyl stretching motions increasing the number of modes involving the methyl groups. In the calculation of Warshel and Karplus (1974), three modes in this region are predicted for 11-*cis*,12-*s*-*cis*-retinal (12-s-trans was not calculated): 1063 and 1000 cm^{-1} both of which involve primarily C–Me stretching and 936 cm^{-1} which is a combination of C–Me stretch and C–C–C bending. In our model the 11-cis crystal data (Figure 3) are then interpreted in terms of this calculation as the following: the 1033 cm^{-1} line represents primarily C(5) methyl stretch, the 1018 cm^{-1} line represents primarily the stretching motions of the methyl groups on C(9) and C(13) which are degenerate, and the 965 cm^{-1} line is the combination methyl stretch and bending mode. In the 11-cis,12-s-trans conformation the degeneracy of the 1018 cm^{-1} is lifted. Whether this simple model represents in detail the actual normal modes must await further theoretical calculations and experimental work. However, the model points out that the 13-Me stretching motion should be significantly modified in the 11-cis,12-s-trans conformation compared with that of 12-s-cis and that this would be reflected in changes in the Raman spectra.

Resonance Raman Spectra of Rhodopsin. The Raman spectra of rhodopsin (Figure 4) support previous (Lewis et al., 1973; Oseroff and Callender, 1974; Mathies et al., 1976) measurements that retinal and opsin are joined by a protonated Schiff base linkage. The position of the 1657 cm^{-1} band in the rhodopsin spectra of Figure 4 is in close correspondence with previous measurements on protonated Schiff bases of retinal model compounds and distinctly far from the values (approximately 1630 cm^{-1}) found for unprotonated Schiff bases of retinal model compounds (Heyde et al., 1971). The position of the C=C stretching mode (1545 cm^{-1}) of the rhodopsin spectrum is somewhat too low to fit exactly the correlation plot of Oseroff and Callender (1974) based on the simple delocalization model. Their fit would predict its position to be near 1550 cm^{-1}. However, as shown above, the C=C frequency of 11-*cis*-retinal is low because of its molecular configuration.

A comparison of the resonance Raman spectra of 9-*cis*-retinal relative to isorhodopsin and 11-*cis*-retinal relative to rhodopsin indicates generally that they have similar spectral features. A detailed analysis and comparison of these spectra in terms of molecular configuration is difficult at the present time; information regarding a precise theoretical analysis of the normal modes, the influence of the terminal end group on the Raman structure, and the degree of resonance Raman enhancement for each mode (which may depend on the exciting laser wavelength) is required. However, one major difference in both visual pigments is the appearance of a line near 1240 cm^{-1} which is absent in the free retinal spectra. On balance, the rhodopsin Raman structure resembles the solution spectra of 11-*cis*-retinal closer than any other isomer and this relation applies similarly for isorhodopsin and 9-*cis*-retinal.

One extremely interesting similarity in the rhodopsin data of Figure 4 compared with the solution 11-*cis*-retinal spectrum is the appearance of two bands at 998 and 1015 cm^{-1}. As discussed above, the 11-*cis*-retinal spectra could be understood by assigning the 998 cm^{-1} band to the stretching modes of 13-Me in the 12-s-trans form and the 1018 cm^{-1} band to 13-Me in the 12-s-cis form and 9-Me in both forms (see Figure 5). By assuming that the chromophore in rhodopsin has a single conformation or that the 9- and 13-Me stretching motions give rise to nearly equal Raman intensities and noting that the 998 and 1015 cm^{-1} band intensities are nearly equal, these data suggest rather strongly that 11-*cis*-retinal in rhodopsin is (perhaps distorted) 12-s-trans rather than the somewhat more stable 12-s-cis form found in crystals.

In contrast to the case of retinal solutions (discussed above) this conclusion is in quite good agreement with the studies of Chan et al. (1974) and Ebrey et al. (1975) on the pigments formed from 11-*cis*-14-methylretinal. In this case, it was found that the 11-cis isomer of this analogue in opsin had very similar absorption and CD structure as well as photosensitivity to that of rhodopsin. Since it is assumed that the conformation of 11-*cis*-14-methylretinal is forced away from the 12-s-cis by steric hindrance, their conclusion is that the conformation of the 12-C/13-C bond of the chromophore in the pigment is different from that of crystalline 11-*cis*-retinal.

Acknowledgments

The idea of controlling the degree of photoisomerization by moving the sample through the laser beam evolved through discussions between one of us (R.H.C.) and Dr. Allan Oseroff at Yale University. We would like to thank Dr. Richard Mathies, Dr. Allan Oseroff, and Professor Lubert Stryer for a preprint of their paper on flow Raman studies of rhodopsin and isorhodopsin. We greatly appreciate the help of Dr. Anthony Yudd with some of the control experiments.

References

Abrahamson, E. W., and Wiesenfeld, J. R. (1972), in Handbook of Sensory Physiology, Vol. VII/1, Dartnall, H. J. A., Ed., Heidelberg, Springer, pp 69–121.

Broersma, S., (1960), *J. Chem. Phys. 32,* 1632.

Chan, W. K., Nakanishi, K., Ebrey, T. G., Honig, B. (1974), *J. Am. Chem. Soc., 96,* 3642.

Ebrey, T., Govindjee, R., Honig, B., Pollock, E., Chan, W.

K., Crouch, R., Yudd, A., and Nakanishi, K. (1975), *Biochemistry 14,* 3933.
Fenstermacher, P. R., and Callender, R. H. (1974), *Opt. Commun. 10,* 181.
Gilardi, R. D., Karle, I. L., and Karle, J. (1972), *Acta Crystallogr. Sect. B 28,* 2605.
Gill D., Heyde, M. E., and Rimai, L. (1971), *J. Am. Chem. Soc. 93,* 6288.
Heyde, M. E., Gill, D., Kiponen, R. G., and Rimai, L. (1971), *J. Am. Chem. Soc. 93,* 6776.
Honig, B., and Ebrey, T. G. (1974), *Annu. Rev. Biophys. Bioeng, 3,* 151.
Honig, B., and Karplus, M. (1971), *Nature (London) 229,* 558.
Landau, L. D., and Lifshitz, E. M. (1959), Fluid Mechanics, London, Pergamon Press, Chapter 2.
Lewis, A., Fager, R. S., and Abrahamson, E. W. (1973), *J. Raman Spectrosc. 1,* 465.
Lewis, A., Spoonhower, J., Bogomoin, R. A., Lozier, R. H., and Stoeckenius, W. (1974), *Proc. Natl. Acad. Sci., U.S.A. 71,* 4462.
Mathies, R., Oseroff, A. R., and Stryer, L. (1976), *Proc. Natl. Acad. Sci. U.S.A. 73,* 1.
Mendelsohn, R. (1973), *Nature (London) 243,* 22.
Mendelsohn, R., Verma, A. L., Berstein, H. J., and Kates, M. (1974), *Can. J. Biochem. 52,* 774.
Oseroff, A. R., and Callender, R. H. (1974), *Biochemistry 13,* 4243.
Papermaster, D. S., and Dreyer, W. J. (1973), *Biochem. 13,* 2438.
Rimai, L., Gill, D., and Parsons, J. L. (1971), *J. Am. Chem. Soc. 93,* 1353.
Rowan, R., Warshel, A., Sykes, B. D., and Karplus, M. (1974), *Biochemistry 13,* 970.
Tang, J., and Albrecht, A. C. (1970), Raman Spectroscopy 2, Chapter 2.
Tennekes, H., and Lumley, J. L. (1972), A First Course in Turbulence, Cambridge, Mass., MIT Press, Chapter 5.
Wald, G. (1967), *Science 162,* 230.
Wald, G. (1968), *Nature (London) 219,* 800.
Warshel, A., and Karplus, M. (1974), *J. Am. Chem. Soc. 96,* 5677.

Reaction Free Energy Surfaces in Myosin–Actin–ATP Systems†

Terrell L. Hill* and Evan Eisenberg

ABSTRACT: If we select for consideration any reaction $M_1 \rightleftarrows M_2$ in the myosin-ATPase cycle, the question arises as to the relations between the rate constants for (1) $M_1 \rightleftarrows M_2$, (2) $AM_1 \rightleftarrows AM_2$ (A = actin), (3) $A + M_1 \rightleftarrows AM_1$, and (4) $A + M_2 \rightleftarrows AM_2$, with actin and myosin either (a) in solution or (b) in the myofilament structure. It is shown here, by means of examples, that a single so-called potential of mean force, W, and structural free energy, A_m, suffice to determine the reaction free energy surfaces for all of these transitions (W for the solution case, $W + A_m$ for the structured case). In fact, A_m is the same for all reactions in the myosin-ATPase cycle. Of course, though indispensable as the starting point and adequate for qualitative understanding, the reaction free energy surface does not provide (without additional theory) the actual values of the rate constants or of the corresponding basic free energy changes in the myosin states involved. These rate constants and free energies are discussed, in a preliminary way, in two other papers.

The kinetics of myosin-ATPase activity is important because of its relation to muscle contraction. This relation is also responsible for the complexity of the subject: myosin-ATPase activity is considerably altered either in the presence of actin in solution or when its locale is the myofilament system of active muscle. From the theoretical side, the first step in trying to understand some of these complications is to visualize the transitions of the myosin-ATPase cycle in terms of reaction free energy surfaces (analogous to the potential surfaces of molecular rate theories). The object of this paper is to discuss the pertinent free energy surfaces in the simplest possible terms, basing the argument on rather arbitrary examples chosen for illustrative purposes only. Our aim is to sketch the essential features involved; the details and choice of examples will certainly need to be altered in the future as more biochemical and structural information becomes available.

In two other papers (T. L. Hill, manuscript in preparation; 1975a), the argument given here will be supplemented in more quantitative terms. This elaboration will include a preliminary discussion of the connections between the reaction free energy surfaces, on the one hand, and the corresponding rate constants and basic free energy levels (Hill and Simmons, 1976) of myosin states, on the other. To put it briefly, contributions must be considered, *other than* from the reaction free energy surface, to both the basic free energies and the activation free energies (see also Hill, 1976).

The present paper is concerned only with free energy surfaces per se. However, these surfaces are the most important single feature involved and are adequate to provide a qualitative understanding of the problem.

† From the Laboratory of Molecular Biology, National Institute of Arthritis, Metabolism, and Digestive Diseases (T.L.H.), and the Laboratory of Cell Biology, National Heart and Lung Institute (E.E.), National Institutes of Health, Bethesda, Maryland 20014. *Received October 6, 1975.*